

# $R_{out}/R_{sid}$ and Opacity at RHIC

Larry McLerran<sup>1</sup> and Sandra S. Padula<sup>1,2</sup>

<sup>1</sup> *Nuclear Theory Group, Brookhaven National Laboratory, Upton, NY 11793, USA*

<sup>2</sup> *Instituto de Física Teórica, Universidade Estadual Paulista, São Paulo - SP, Brazil;  
 Theoretical Physics, FERMILAB, Batavia, IL 60510, USA*

## Abstract

One of the most dramatic results from the first RHIC run are the STAR results for  $\pi^\pm\pi^\pm$  interferometry. They showed that the ratio of the so-called  $R_{out}$  and  $R_{sid}$  radii seem to decrease below unity for increasing transverse momentum of the pair ( $K_T$ ). This was subsequently confirmed by PHENIX. We consider here the effects of opacity of the nuclei on this ratio, and find that such a small value is consistent with surface emission from an opaque source.

## I. INTRODUCTION

The striking result on  $\pi^\pm\pi^\pm$  by STAR Collaboration [1] is not yet understood for  $R_{out}/R_{sid}$ . This is the ratio of the radius measured in the correlation along the direction of the sum of the particle's momentum divided by the correlation perpendicular to the beam and perpendicular to the outwards direction. This result was subsequently confirmed by PHENIX [2]. In an attempt to understand this result we consider in detail a generalization of the model used by Heiselberg [3] to include effects of source opacity at CERN energies.

The origin of the problem can be understood from the simplest model of HBT [4]. In this model we let particles be emitted from the entire volume of the system. In this case, the spatial size which is probed by  $R_{out}$  and  $R_{sid}$  is of the same order of magnitude, the radius of the system. However,  $R_{out}$  also has a spatial correlation built in on account of the time differences of different emissions [5].  $R_{out}$  is the size scale measured along the particle's direction of motion. Particles emitted at much different times end up spatially separated from one another in this direction. We therefore expect that since the time separations are of the order of the size of the system (which for practical purposes seems to be a reasonable approximation for order of magnitude estimates at RHIC), then  $R_{out}/R_{sid} > 1$ . Most simple models incorporating the above physics give the ratio to be about  $R_{out}/R_{sid} \sim 2$ .

The assumption that the particles are emitted from the entire volume of the system is probably a bad one. Data on  $p_T$  distributions of particles in STAR [1] and PHENIX [2] suggest that the system is opaque to particles up to large transverse momenta. A more reasonable description might be blackbody surface emission.

To implement opacity, we consider a model where the matter is emitting from a surface at a fixed radius. The system is allowed to undergo 1+1 dimensional longitudinal expansion. The details of this model and its results are described in the fourth section.

An important ingredient of this model is decoupling, which we assume occurs at a well defined temperature. In the surface emission model we use, this requires the decoupling to occur throughout the transverse volume of the system at a well defined time. This therefore contributes to  $R_{out}/R_{sid} \sim 1$ , since there is no enhancement due to a distribution of times.

In the second section, before turning to explicit model computations, we review the method of the Covariant Current Ensemble formalism for computing two particle HBT correlation functions. In this section, we try to be general enough to include the physics needed for our various computations.

In the third section, we consider a simpler version of the above model. We compute the various radii for the case of a cylinder emitting at a constant temperature  $T$  for a finite time  $\Delta t$ . We will consider both the case of an opaque source and a transparent one. In this oversimplified model, we show that in the opaque source limit, that  $R_{out} \sim \sqrt{\Delta t^2 + (0.2R_T)^2}$  and  $R_{sid} \sim R_T$ . For the realistic case where  $\Delta t \sim R_T$ ,  $R_{out}/R_{sid} \sim \Delta t/R_T$ , and this ratio can be less than one. In the transparent limit  $R_{out} = \sqrt{\Delta t^2 + R_T^2}$  and  $R_{sid} \sim R_T$ , this ratio is always larger than 1.

In the heavy ion experiments, the ratio  $R_{out}/R_{sid}$  is larger than 1 at AGS to SPS energies for  $\pi^-\pi^-$  pairs [6,7]. For  $\pi^+\pi^+$  it is also larger than 1 at AGS ( $R_{out}/R_{sid} \approx 1.3$  - E859 Collab. [6,8]) but slightly smaller than 1 at SPS, according to NA44 data [6], although it is bigger than 1 for  $\pi^-\pi^-$ . It is interesting to look at the results shown in Ref. [7] for NA49 data, since they fit the same data sample with Gaussian Cartesian parameterization (obtaining the fits in terms of  $R_{out}$ ,  $R_{sid}$ , and  $R_{long}$ ), as well as with the so-called Yano-Koonin-Podgoretskii one, i.e. (see Ref. [6] for details),

$$C(\mathbf{q}, \mathbf{K}) = 1 + \exp \left[ R_\perp^2 q_\perp^2 - R_\parallel^2 Z(q_\parallel^2 - q_0^2) - (R_0^2 + R_\parallel^2)(q \cdot U)^2 \right],$$

from where we see that the variable  $R_0$  is related to the time coordinate. The variable  $R_{out}$  should therefore be approximately  $R_{out} = \sqrt{R_\perp^2 + R_0^2}$ . The velocity parameter  $U(\mathbf{K}) = \gamma(\mathbf{K})(1, 0, 0, v(\mathbf{K}))$  and  $q_\perp = \sqrt{q_{out}^2 + q_{sid}^2}$ . We show the values for  $R_{out}$ ,  $R_{sid}$ , as well as for  $R_\perp$ , and  $R_0$ , in Table 1 below [6].

**TABLE 1: Results from CERN/SPS NA49 data fitted both with the Gaussian Cartesian and Yano-Koonin-Podgoretskii parameterizations.**

$\langle K_T \rangle$ (GeV/c)	0.065	0.151	0.247	0.365
$R_{out}$ (fm)	$6.22 \pm 0.17$	$6.23 \pm 0.26$	$5.80 \pm 0.39$	$5.51 \pm 0.47$
$R_{sid}$ (fm)	$5.77 \pm 0.35$	$5.20 \pm 0.34$	$5.00 \pm 0.18$	$4.63 \pm 0.27$
$R_{out}/R_{sid}$	$\approx 1.08$	$\approx 1.20$	$\approx 1.16$	$\approx 1.19$
$R_0$ (fm)	$5.3 \pm 1.7$	$3.8 \pm 1.2$	$2.9 \pm 1.2$	$2.8 \pm 1.0$
$R_\perp$ (fm)	$5.72 \pm 0.41$	$5.33 \pm 0.31$	$5.10 \pm 0.35$	$4.82 \pm 0.57$
$\sqrt{(R_\perp^2 + R_0^2)}$ (fm)	$7.8 \pm 2.6$	$6.6 \pm 2.1$	$5.9 \pm 2.4$	$5.6 \pm 2.1$

Although the error bars in  $R_0$  from NA49 data [6] above are very big, which propagates to the estimate on the last line of the Table 1 above, we see that, indeed, the value of

$\sqrt{(R_\perp^2 + R_0^2)}$  is compatible with the corresponding values for  $R_{out}$  within the same data set, as would be expected, which makes the ratio  $R_{out}/R_{sid}$  to be above unity.

Although the value of  $R_{out}/R_{sid}$  is above one at the AGS, it is relatively close to one at the SPS, and the data at RHIC gives an even smaller value. This suggests that at RHIC this ratio reflects the opacity of the emitting surface. The origin of the smaller value of  $R_{out}/R_{sid}$  for the opaque case is due to two effects. First, the system radiates from a smaller geometrical region than in the transparent case. Second, the emission itself is preferentially from the region of the cylinder closest to the radial vector made by  $\mathbf{R}_{out}$ . This is because radiation from this region is normal to the surface, and there is a factor of  $\cos(\phi)$  associated with the flux in the direction of  $\mathbf{R}_{out}$ , where  $\phi$  is the angle between  $\mathbf{R}_{out}$  and a normal vector to the surface. Finally there is also the emission from the decoupling surface which occurs at a well defined time and therefore contributes  $R_{out}/R_{sid} \sim 1$

The case of  $1 + 1$  dimensional longitudinal expansion is more complicated. In later sections, we shall use a simple model of the matter, where there is a real first order phase transition between a parton (gluons and massless quarks) gas and a pion gas. The energy is emitted from the partonic phase. This quark and gluon matter is assumed to be directly converted into a flux of pions with the same energy and a blackbody distribution at the temperature of emission. This energy conservation condition allows us to directly take a flux of gluons and quarks and convert it into a spectrum of pions. It of course will mess up details of the fragmentation, and generates some increase in entropy, but for our purposes such a crude treatment is sufficient to demonstrate the physics of opacity in a semi-quantitative way. The emission of the hadron degrees of freedom is taken to be entirely pions. We will find that the dominant emission at RHIC energies comes from times after the beginning of the mixed phase, but there is a significant mixture of gluonic and quark radiation which must convert into pions.

The characteristic time scale for emission is of the order of the radius of the system before the radiation is significantly attenuated. This time scale is of the order of the size of the system for RHIC energies. Our model which incorporates this physics is described in detail in Sec. 4. In the fifth section, we describe some of the details of the computation of the HBT correlation function.

In the final section, we discuss the limitations of our approach. The severest is that if we try to predict the values of HBT radii as a function of  $K_T$  of the pair, we do not get the correct transverse momentum dependence. We do however get the correct  $K_T$  dependence for  $R_{out}/R_{sid}$ . The most likely reason we do not get the absolute HBT radii and their dependence upon time is that the radius of the system is time dependent. This time dependence is correlated with the temperature of the system and hence a correlation is generated between pair transverse momentum and time. We could model this, but this goes beyond the scope of what we intended to do, which was merely to give some insight into the experimentally observed values of  $R_{out}/R_{sid}$ . The ratio of  $R_{out}/R_{sid}$  should only be weakly dependent upon the absolute values of  $R_{sid}$  and  $R_{out}$  since it is dimensionless, and since we expect that the characteristic emission time will scale with the size of the system  $R_{sid}$ , that is the ratio should roughly scale as  $R_{sid}$  and the emission time change in tandem. Of course, getting the details of this correctly involves a much more detailed computation, and this may reveal other weaknesses of the standard space-time description of heavy ion collisions.

## II. THE COVARIANT CURRENT ENSEMBLE INPUTS

To compute the emitted spectrum and the two particle distribution function, which leads to the interferometry relations in which we are interested, we consider the Covariant Current Ensemble formalism, [10], [11]. In this formalism, the two particle correlation function can be written as

$$C(k_1, k_2) = \frac{P_2(k_1, k_2)}{P(k_1)P(k_2)} = 1 + \frac{|G(k_1, k_2)|^2}{G(k_1, k_1)G(k_2, k_2)} \quad (1)$$

where  $P_1(k_i)$  and  $P(k_1, k_2)$  are, respectively, the single particle distribution and the probability for simultaneous observation of two particles of momentum  $k_1, k_2$ .

The complex amplitude,  $G(k_1, k_2)$ , is written as

$$G(k_1, k_2) = \int d^4p \int d^4x e^{iq^\mu x_\mu} D(x, p) j_0^*(\frac{k_1 \cdot p}{m}) j_0(\frac{k_2 \cdot p}{m}) , \quad (2)$$

and the single-inclusive distribution,  $G(k_i, k_i)$ , is written as

$$G(k_i, k_i) = \int d^4p D(0, k_i) |j_0(\frac{k_i \cdot p}{m})|^2 = \frac{d^3\mathcal{N}}{dk^2 dy} = E \frac{d^3\mathcal{N}}{dk^3} = P_1(k) . \quad (3)$$

We see that

$$D(q, k) = \int d^4x e^{iq^\mu x_\mu} D(x, k) . \quad (4)$$

where  $D(x, k)$  is the normalized phase-space distribution at the instant of the emission.

There are several different possibilities for  $D(x, k)$ :

The first is radiation from a transparent cylinder which is not expanding in the transverse directions and has no longitudinal expansion.

$$D(x, k) = g_p C_\tau \exp(-t^2/2\Delta t^2) \delta(E_p - p^0) \delta^2(\mathbf{p}_T) \delta(p_z) . \quad (5)$$

In this expression  $p$  is to be interpreted as the momentum of a particle at rest in the matter from which it is emitted, and reflects the collective motion of the system. For matter at rest,  $\mathbf{p} = 0$ . The factor  $g_p$  counts the number of degrees of freedom of particle being emitted. The factor of  $e^{-t^2/2\Delta t^2}$  is a Gaussian parameterization of the source emission rate, so that the characteristic emission time is  $\Delta t$ . (The blackbody rate emerges naturally in this picture, and  $C_\tau$  is a factor which modifies beyond the blackbody rate).

The second case is emission from the surface of a cylinder without longitudinal expansion. Here we must account for the fact that the particle is emitted with a flux factor which depends upon the angle  $\phi$  which is between the normal vector to the surface and the direction  $\mathbf{x}$ . There is also a factor of  $\delta(r - R)$  which requires that particles are emitted from the surface and a factor of  $\Theta(\cos(\phi))$  which requires they come from the side of the surface from which they are emitted.

$$D(x, k) = g_p C_\tau \exp(-t^2/2\Delta t^2) \delta(r_T - R_T) \delta(E_p - p^0) \delta^2(\mathbf{p}_T) \delta(p_z) \cos \phi \Theta(\cos \phi) . \quad (6)$$

Finally, there is the case of emission from the surface of a cylinder with longitudinal expansion

$$D(x, k) = g_p \kappa C_\tau \delta(r_T - R_T) \delta(E_p - p^0) \delta^2(\mathbf{p}_T) \rho(y) \delta(y - \eta) \cos \phi \Theta(\cos \phi) , \quad (7)$$

where  $\rho(y)$  is the rapidity distribution of the system (supposed to be uniform in Bjorken model). The factor of  $\delta(y - \eta)$  is the correlation between the velocity and coordinate of the emitting surface built into the Bjorken model [9]. The factor of  $C_\tau$  controls the rate of emission from the surface as a function of time. We will fix this by requiring the system to be either a Quark Gluon Plasma, a hadron gas or a mixture, with blackbody radiation and the mixture determined by thermodynamics.

The currents correspond to thermal distributions and are written as

$$j_0\left(\frac{k_i \cdot p}{m}\right) = \sqrt{u^\mu k_{i\mu}} \exp\left\{-\frac{u^\mu k_{i\mu}}{2T(\tau)}\right\} . \quad (8)$$

Here  $u^\mu = p^\mu/m$  is the four vector flow velocity which is the four velocity of the emitting surface. In the above,  $u^\mu = (1, \mathbf{0})$ . We indicate by  $T(\tau)$  the dependence of the temperature in the proper time,  $\tau$ , prior to the beginning of the mixed phase, as given by Eq.(19).

In Bjorken picture with no transverse flow, the 4-velocity  $u^\mu$  and the momentum of the emitted particle,  $k^\mu$ , can be written as

$$u^\mu = (\cosh \eta, 0, 0, \sinh \eta) ; k^\mu = (m_T \cosh y, \mathbf{k}_T, m_T \sinh y) . \quad (9)$$

In our study of the effects of (constant) flow below, we will assume that the 4-velocity  $u^\mu$  is written as

$$u^\mu = \cosh \eta_T (\cosh \eta_L, \mathbf{v}_T, \sinh \eta_L) . \quad (10)$$

In this equation  $\gamma_T = \cosh(\eta_T) = 1/\sqrt{1 - v_T^2}$  is the transverse space-time rapidity.

In this case, instead of the two-dimensional delta function,  $\delta^2(\mathbf{p}_T)$  in Eq. (5)-(7), we may write the transverse momentum part of the phase-space distribution as

$$g(\mathbf{p}_T) = \delta^2(\mathbf{p}_T - m\mathbf{u}_T) . \quad (11)$$

In our model, we shall only need the flow velocity at the surface, and hence the simple form above. When we consider flow, we shall take  $u_T$  to be a constant independent of time, again a tremendous oversimplification, but sufficient to make our point.

### III. A VERY SIMPLE MODEL FOR $R_{OUT}/R_{SID}$ .

We first work out the simplest model for emission so that we can get some conceptual understanding of the physics involved in the various cases. First consider emission from a transparent cylinder. A little algebra gives

$$C_{out} = 1 + \exp\left[-\frac{K_T^2 q_{out}^2 \Delta t^2}{(K^2 + m^2)}\right] [2J_1(q_{out} R_T)/(q_{out} R_T)]^2 \quad (12)$$

and

$$C_{sid} = 1 + [2J_1(q_{sid} R_T)/(q_{sid} R_T)]^2 , \quad (13)$$

where  $J_1(x)$  is the Bessel function of the first kind and order one.

In this equation, it is absolutely clear that  $R_{out} > R_{sid}$ , and that if  $\Delta t \sim R$ , then  $R_{out} \sim 2R_{sid}$

Now let us consider the result for surface emission. In this case, a little algebra yields

$$C_{out} = 1 + \exp \left[ -\frac{K_T^2 q_{out}^2 \Delta t^2}{(K^2 + m^2)} \right] |I(q_{out} R_T)|^2 \quad (14)$$

where

$$I(x) = \frac{1}{2} \int_0^\pi d\phi \sin(\phi) \exp(ix \sin(\phi)) \quad (15)$$

On the other hand,

$$C_{sid} = 1 + \left| \frac{\sin(q_{sid} R_T)}{(q_{sid} R_T)} \right|^2 \quad (16)$$

In Fig. 1, we plot  $C_{sid}$  and the pieces of  $C_{out}$  which does not involve the time  $\Delta t$ . Fitting the curves, we find that, in the opaque case,  $R_{sid}^{eff} \approx R_T \times 0.53$  and  $R_{out}^{eff} = \sqrt{\Delta t^2 + (R_T \times 0.22)^2}$ . In the transparent case, the fit results in an effective radius of  $\approx 0.61 R_T$ .

The basic result we get from this analysis is that for the opaque cylinder, unlike the transparent one, we can easily have  $R_{out} < R_{sid}$ . In fact for  $R_{out} \sim \Delta t$ , the ratio of  $R_{out}/R_{sid} \sim \Delta t/R_T$  unlike the transparent cylinder case where  $R_{out}/R_{sid} \sim \sqrt{\Delta t^2 + R_T^2}/R_T$ .

#### IV. A SIMPLE MODEL FOR $R_{OUT}/R_{SID}$

In this model, we incorporate longitudinal expansion. Here the system cools as it expands, so we need to have the rate of emission vary as a function of time.

We need to have dynamical description of the microphysics to be able to do this. Our more or less conventional model is a Quark-Gluon Plasma (QGP) phase at some temperature above the critical temperature,  $T_0 > T_c$ . It goes into a mixed phase of QGP and hadron gas at the critical temperature, and we take this hadronic gas to be composed of an ideal gas of pions. Below  $T_c$ , it a gas of pions. The system subsequently cools until it reaches a decoupling temperature. We choose this critical temperature to be 175 MeV to be consistent with lattice Monte-Carlo data. We choose the decoupling temperature to be  $T_f = 150$  MeV to be consistent with the typical energy per particle observed in the RHIC experiments, and to fit the observed  $p_T$  distributions of pions. However, these values chosen for  $T_c$  and  $T_f$  are not crucial for qualitatively reproducing the results we discuss here, since they are only weakly sensitive to these particular values.

The system produced in a heavy ion collision will expand and the temperature will gradually decrease. The initial expansion is in a Quark-Gluon Plasma, and the system expands longitudinally. After this initial stage, lasting about  $(\tau_c - \tau_0)$ , the transition temperature,  $T_c$ , is reached and the evolution, which takes a relatively long time, begins in the mixed phase, during which the temperature remains constant with time. The mixed phase continues for such a long period that when it ends, after an elapsed interval  $(\tau_h - \tau_c)$ , the system is quite

dilute, and much of the particle have been evaporated from the surface of the system by this time. It then begins an expansion as a pion gas until the decoupling temperature is reached.

The Bjorken hydrodynamical model [9] should be able to describe the system during its evolution from formation until the time it breaks up. We will supplement this with radiation from the surface of the matter. We will take the radius at which this radiation takes place to be a constant and the radius of the nuclei. We only consider impact parameter zero collisions. In realistic hydrodynamic simulations, there is some surface from which the system decouples, and the radius of this surface has some time dependence. It is relatively weak, but this will nevertheless keep us from getting a proper description of the details of the radii as a function of  $p_T$ , which is a measure of the time dependence since the more energetic particles are emitted earlier. The main purpose of this paper is however to study  $R_{out}/R_{sid}$ , and this should be weakly dependent upon the absolute value of the radii. For emission from the surface, we consider both cases of no transverse flow and a constant one defined by a parameter,  $v_0$ .

Another ingredient in our model is the hypothesis that the system will emit from its external surface similarly to a black-body, starting shortly after being formed, at  $\tau = \tau_0$ . In this way, quark and gluon degrees of freedom have to be considered in the QGP and mixed phases. The hadronic degrees of freedom should, in principle, include a complete set of resonances later decaying into pions. However, in this initial description, and for the sake of simplicity, we will consider a hadronic gas constituted of only pions. No complex mechanism for the QGP hadronization will be considered in detail at this point, although hadronization must take place. In other word, in first approximation, we will consider the evaporation of “gluons” and “quarks” (as hadronized pions) from the external surface of the system in the same way as emission of pions, except for the number of degrees of freedom.

We can estimate the emitted energy as well as the total entropy associated to each stage, i.e., from the time the system is formed, at  $\tau = \tau_0$ , in a QGP phase, up to the time it reaches the first order phase transition, at  $\tau = \tau_c$ . This ends after a period  $(\tau_h - \tau_c)$  is elapsed and all the remnant QGP is converted into pions, at  $\tau = \tau_h$ . From that time on, the system continues to evaporate and emit particles up to an instant  $\tau = \tau_f$ , when it is so dilute that decouples. We can then describe the radiated energy and entropy corresponding to each of these stages.

In the initial phase, we can estimate the emitted energy as a function of time considering the emission by an expanding cylinder of transverse radius  $R_T$  and length  $h$ , in a certain time interval between  $\tau$  and  $\tau + d\tau$  by

$$dE_{in} = -\kappa\sigma T^4 2\pi R_T h d\tau - \frac{4}{3} \sigma T^4 \pi R_T^2 dh , \quad (17)$$

where the first term comes from the black-body type of energy radiated from the surface of the cylinder, and the second term results from the mechanical work due to its expansion. The  $\kappa$  factor was introduced to take into account that the system has some opacity to surface emission. The constant  $\sigma$  is the Steffen-Boltzmann constant and is proportional to the number of degrees of freedom in the system.

By integrating that expansion we get for the energy density (i.e.,  $\epsilon = E/V$ )

$$\epsilon_{in} = \epsilon_0 \left( \frac{\tau_0}{\tau} \right)^{\frac{4}{3}} e^{-\frac{2\kappa}{R_T}(\tau - \tau_0)} . \quad (18)$$

From the above expression we see that we obtain an extra multiplicative factor,  $e^{-\frac{2\kappa}{R_T}(\tau-\tau_0)}$ , in addition to that coming from the Bjorken picture. Remembering that, in the Bjorken picture, the relation between the energy density,  $\epsilon$ , and the energy,  $E$ , is given by  $\epsilon/\epsilon_0 = \tau_0/\tau$ , and that  $E = \sigma T^4$  for a blackbody-type radiation, then the variation of the temperature in the initial stage, i.e., prior to the beginning of the phase transition, follows immediately as

$$T(\tau) = T_0 \left( \frac{\tau_0}{\tau} \right)^{\frac{1}{3}} e^{-\frac{2\kappa}{R_T}(\tau-\tau_0)} . \quad (19)$$

The initial entropy can be estimated by

$$s_{in} = \frac{S_{in}}{V} = \frac{1}{T}(\epsilon + p)_{in} = s_0 \left( \frac{\tau}{\tau_0} \right) e^{-\frac{3\kappa}{R_T}(\tau-\tau_0)} \rightarrow S_{in} = S_0 e^{-\frac{3\kappa}{R_T}(\tau-\tau_0)} , \quad (20)$$

where  $s_0 = \frac{4}{3}(\sigma\epsilon_0^3)^{1/4}$  is the initial entropy density.

On the other hand, the entropy associated with the emission can be estimated by

$$\frac{dS_{in}}{V} = \frac{2\kappa}{R_T} s_{in} d\tau = \frac{2\kappa}{R_T} s_0 \left( \frac{\tau}{\tau_0} \right) e^{-\frac{3\kappa}{R_T}(\tau-\tau_0)} \rightarrow S_{emit} = \frac{4}{3} S_0 [1 - e^{-\frac{3\kappa}{R_T}(\tau-\tau_0)}] , \quad (21)$$

which results in the total entropy of the initial stage as being

$$S_{tot} = \frac{4}{3} S_0 - \frac{1}{3} S_0 e^{-\frac{3\kappa}{R_T}(\tau-\tau_0)} , \quad (22)$$

so that, at  $\tau = \tau_0 \rightarrow S_{tot} = S_0$ . Note that this result requires that there be entropy produced during the emission from the surface.

During the phase transition, the energy and entropy can be estimated similarly, leading to

$$\tilde{E}_{emit} = \tilde{E}_c (1 - e^{-\frac{2\kappa}{R_T}(\tau-\tau_c)}) ; \quad \tilde{S}_{in} = \tilde{S}_c e^{-\frac{2\kappa}{R_T}(\tau-\tau_c)} ; \quad \tilde{S}_{emit} = \tilde{S}_c (1 - e^{-\frac{2\kappa}{R_T}(\tau-\tau_c)}) . \quad (23)$$

From the above relations we can see that, during the phase transition, the total entropy,  $\tilde{S}_{tot} = \tilde{S}_{in} + \tilde{S}_{emit} = \tilde{S}_c$  is conserved. During this extended period, the temperature remains constant with time ( $T = T_c$ ), so that the previous relation in Eq. (19) no longer holds.

During the phase transition the system is in a mixed phase of Quark-Gluon Plasma and hadronic gas. If the fraction of the fluid in the QGP phase is  $f$ , then in the hadronic (pion) phase it would be  $(1 - f)$ . On the other hand, from Eq. (23), we see that the portion of the entropy density still in the system is given by  $\tilde{s}_{in} = \tilde{s}_c \left( \frac{\tau_c}{\tau} \right) \exp \left[ -\frac{2\kappa}{R_T}(\tau - \tau_c) \right]$ . Consequently,  $\tilde{s}_{in} = f \tilde{s}_{QGP} + (1 - f) \tilde{s}_h$ , where  $\tilde{s}_{in}(\tau_c) = \tilde{s}_c$  and  $\tilde{s}(\tau_h) = \tilde{s}_c \left( \frac{\tau_h}{\tau_c} \right) \exp \left[ -\frac{2\kappa}{R_T}(\tau_h - \tau_c) \right]$ . If we substitute these expressions into that for  $\tilde{s}_{in}$ , we then get

$$f = \left( \frac{\tau_h e^{-\frac{2\kappa}{R_T}(\tau-\tau_c)} - \tau e^{-\frac{2\kappa}{R_T}(\tau_h-\tau_c)}}{\tau_h - \tau_c e^{-\frac{2\kappa}{R_T}(\tau_h-\tau_c)}} \right) \frac{\tau_c}{\tau} ; \quad (1 - f) = \left( \frac{\tau - \tau_c e^{-\frac{2\kappa}{R_T}(\tau-\tau_c)}}{\tau_h - \tau_c e^{-\frac{2\kappa}{R_T}(\tau_h-\tau_c)}} \right) \frac{\tau_h}{\tau} . \quad (24)$$

Finally, we need to estimate the initial values  $T_0$  and  $\tau_0$ , as well as the proper time,  $\tau_c$ , corresponding to the on-set of the phase transition. We estimate  $\tau_0$  by means of the Uncertainty Principle, i.e.,  $E_0 \tau_0 \approx 1$ , and by

$$E_0 \sim \frac{\int dp \, p^3 \, e^{-p/T_0}}{\int dp \, p^2 \, e^{-p/T_0}} \sim 3T_0 \quad , \quad (25)$$

from which we easily determine the initial time as

$$\tau_0 \sim \frac{1}{3T_0} (GeV^{-1}) \sim \frac{0.197}{3T_0} (fm) \quad . \quad (26)$$

On the other hand, the constraint on  $T_0$  and  $\tau_0$  has to come from the experiment. At RHIC, the average produced multiplicity of pions is  $\mathcal{N} \sim 1000$ , which should be proportional to the initial entropy,  $S_0$ , i.e.,

$$\mathcal{N} = \Gamma S_0 = \Gamma \left[ (g_g + g_q) \times \left( \frac{4}{3} \frac{\pi^2}{30} T_0^3 \right) \right] \pi R_T^2 \tau_0 \quad . \quad (27)$$

In the above expression, the degeneracy factors,  $g$ , are given by the gluon degrees of freedom,  $g_g = 2(\text{spin}) \times 8(\text{color})$ , and the quark/anti-quark degrees of freedom,  $g_q = \frac{7}{8}[2(\text{spin}) \times 2(q + \bar{q}) \times 3(\text{color}) \times N_f(\text{flavor})]$ . In the case of pions, the degeneracy factor would be  $g_\pi = 3$ .

From Eq.(26) and (27) we can determine  $T_0$  as

$$T_0 = \sqrt{\frac{\mathcal{N}}{\Gamma}} \left[ (g_g + g_q) \times \frac{4\pi^3}{270} \frac{R_T^2}{(0.197)^2} \right]^{-1/2} (GeV) \quad . \quad (28)$$

As an example, if we take  $\Gamma = 1$  (and it is indeed expected to be  $\mathcal{O}(1)$ ), then  $T_0 \sim 217$  MeV and  $\tau_0 \sim 0.303$  fm.

For estimating the instant corresponding to the beginning of the mixed phase,  $\tau_c$ , we consider Eq.(19) at  $\tau = \tau_c$ , resulting in

$$\tau_c e^{\frac{3\kappa}{2R_T} \tau_c} = \left( \frac{T_0}{T_c} \right)^3 \tau_0 e^{\frac{3\kappa}{2R_T} \tau_0} \quad , \quad (29)$$

which can be numerically estimated for fixed values of  $\kappa$  and  $T_c$  (for this, we will consider  $T_c = 175$  MeV).

In order to estimate the instant corresponding to the end of the mixed phase,  $\tau_h$ , we need to know  $\tilde{s}_c$  and  $\tilde{s}_h$ . For the first one, we consider a system of gluons and (massless) quarks forming an ideal gas, resulting in  $\tilde{s}_c = (g_g + g_q) \frac{2\pi^2}{45} T_c^3$ . For estimating  $\tau_h$ , we consider the pions as massless particles, while in the system, leading to  $\tilde{s}_h = g_\pi \frac{2\pi^2}{45} T_c^3$ . Then, equating the expression for  $\tilde{s}_{in}$  at  $\tau = \tau_h$ , we obtain

$$\tau_h e^{\frac{2\kappa}{R_T} \tau_h} = \left( \frac{g_g + g_q}{g_\pi} \right) \tau_c e^{\frac{2\kappa}{R_T} \tau_c} \quad , \quad (30)$$

which can be estimated numerically for a fixed value of  $\kappa$ , since  $\tau_c$  was already determined by Eq. (29).

We assume that, at the end of the phase transition, corresponding to  $\tau = \tau_h$ , the system is an ideal gas of pions (no resonances are considered in this initial estimate), which continues to expand and cool down, until the temperature drops to  $T_c = 150$  MeV, corresponding to

an instant  $\tau = \tau_f$ . At this point, whatever is remnant of the system breaks up. The portion of the pions still in the system at that time we call  $\mathcal{F}$ , i.e., the fraction of the system that is emitted at the time  $\tau_f$ . This breakup instant can be estimated by an expression similar to Eq.(19)), with  $T_0$  replaced by  $T_c$ , and  $\tau_0$  by  $\tau_c$ , resulting in

$$\tau_f e^{\frac{3\kappa}{2R_T}\tau_f} = \left(\frac{T_c}{T_f}\right)^3 \tau_h e^{\frac{3\kappa}{2R_T}\tau_h} , \quad (31)$$

which can be numerically estimated for fixed values of  $\kappa$ ,  $T_c$ , and  $T_f$ , and corresponding  $\tau_h$ .

We illustrate in Table 2 below these variables for two different assumptions on  $\kappa$ . The values of the temperatures considered were  $T_0 \sim 217$  MeV (obtained from Eq. (28)),  $T_c = 175$  MeV and  $T_f = 150$  MeV. We also include the corresponding estimates of the remnant flux at  $\tau_f$ ,  $\mathcal{F}$ .

**TABLE 2: Values of the proper-time parameters  $\tau_0$ ,  $\tau_c$ ,  $\tau_h$ ,  $\tau_f$ , as well as of the remaining flux at  $\tau_f$ , for two values of  $\kappa$ .**

$\kappa$	$\tau_0$ (fm/c)	$\tau_c$ (fm/c)	$\tau_h$ (fm/c)	$\tau_f$ (fm/c)	$\mathcal{F}$ at $\tau_f$ (remaining flux)
1	0.303	0.547	3.18	4.12	0.320
1/2	0.303	0.561	4.14	5.62	0.460

To estimate the remnant flux at  $\tau_f$ ,  $\mathcal{F}$ , we have subtracted from the total number of particles given in Eq. (27), the fraction already emitted in the interval  $\tau_0 < \tau \leq \tau_c$ , plus the fraction then emitted in the interval  $\tau_c < \tau \leq \tau_h$ , and finally, in the subsequent period  $\tau_h < \tau \leq \tau_f$ . The fraction of the total number of particles ( $\mathcal{N}$ ) emitted in the first period is given by

$$\frac{\mathcal{N}_1}{\mathcal{N}} = \frac{4}{3} (1 - e^{-\frac{3\kappa}{2R_T}(\tau_c - \tau_0)}) . \quad (32)$$

Similarly, the fraction  $\mathcal{N}_2/\mathcal{N}$  emitted during the phase transition is written as

$$\frac{\mathcal{N}_2}{\mathcal{N}} = e^{-\frac{3\kappa}{2R_T}(\tau_c - \tau_0)} (1 - e^{-\frac{2\kappa}{R_T}(\tau_h - \tau_c)}) . \quad (33)$$

Finally, the fraction emitted during the pion phase, prior to reaching  $T_f$ , can be estimated by

$$\frac{\mathcal{N}_3}{\mathcal{N}} = \frac{4}{3} (1 - e^{-\frac{3\kappa}{2R_T}(\tau_c - \tau_0)}) e^{-\frac{2\kappa}{R_T}(\tau_h - \tau_c)} (1 - e^{-\frac{3\kappa}{2R_T}(\tau_f - \tau_h)}) . \quad (34)$$

Consequently, the remnant fraction at  $\tau = \tau_f$ ,  $\mathcal{F}$ , whose numerical values are written in Table 2, is given by

$$\mathcal{F} = 1 - \frac{1}{\mathcal{N}}(\mathcal{N}_1 + \mathcal{N}_2 + \mathcal{N}_3) . \quad (35)$$

We show in Fig. 2 the evolution of the emitted flux with proper time. The two different cases correspond to different surface emissivities. The curves end at the decoupling temperature. In the case of the greatest rate of surface emission, about 70% of the radiation comes from the surface and the rest from the decoupling volume. It is about 50% for the other case we show for illustration. In the first case, the system decouples at a time of about 4 fm/c and in the second case at about 6 fm/c. We assume a decoupling temperature of 150 MeV.

## V. SINGLE- AND TWO-PARTICLE PROBABILITY DISTRIBUTIONS

We define the average momentum of the pair as  $K = \frac{1}{2}(k_1 + k_2)$  and the relative momentum as  $q = (k_1 - k_2)$ . They satisfy  $q^\mu K_\mu = 0$ , and, consequently, the temporal component of  $q^\mu$  can be written as  $q^0 = \frac{\mathbf{q} \cdot \mathbf{K}}{K^0}$ . In the limit that is interesting for interferometry, we can consider  $|\mathbf{q}| \ll |\mathbf{K}|$ , which implies that  $K^0 \approx \sqrt{|\mathbf{K}|^2 + m^2} = E_K$ .

In both expressions for  $C(k_1, k_2)$  and  $C(k_i, k_i)$ , we see that, due to the form of the phase distribution in Eq.(7), the integration over the variables involving delta functions are straightforward. We should remember that the integration over  $d\phi$  runs in the interval  $[-\pi/2, \pi/2]$ , while the limits on the proper time integration would be  $[\tau_0, \tau_f]$ . However, as the system has different composition in each phase, we should split this time integration to be  $[\tau_0, \tau_c]$ ,  $[\tau_c, \tau_h]$ , and then  $[\tau_h, \tau_f]$ . The rapidity integration should run, in the Bjorken picture, from  $(-\infty, +\infty)$ .

We recall that  $f$  and  $(1 - f)$  are, respectively, the fractions of the system in the QGP phase and in the hadronic phase, according to the expression given in Eq.(24). Then, by taking into account the above observations, the expression for the complex amplitude, after some algebraic manipulation, can finally be written as

$$\begin{aligned}
G(k_1, k_2) = & \langle \rho(y) \rangle C_\tau R_T \int_{-\frac{\pi}{2}}^{\frac{\pi}{2}} d\phi \cos \phi \int_{-\infty}^{+\infty} dy [E_K \cosh y - K_L \sinh y] \\
& e^{-iq_T R_T \cos(\alpha - \phi)} \left\{ \frac{g_{QGP}}{g_\pi} \int_{\tau_0}^{\tau_c} \tau d\tau e^{i\tau[\frac{K_T}{E_K} q_T \cos \alpha \cosh y + q_L (\frac{K_L}{E_K} \cosh y - \sinh y)]} \right. \\
& \exp \left[ -\frac{1}{T_0} (E_K \cosh y - K_L \sinh y) \left( \frac{\tau}{\tau_0} \right)^{1/3} e^{\kappa(\tau - \tau_0)/(2R_T)} \right] + \frac{g_{QGP}}{g_\pi} \times \\
& \int_{\tau_c}^{\tau_h} \tau d\tau (f) e^{i\tau[\frac{K_T}{E_K} q_T \cos \alpha \cosh y + q_L (\frac{K_L}{E_K} \cosh y - \sinh y)]} e^{-\frac{1}{T_c} (E_K \cosh y - K_L \sinh y)} + \\
& \int_{\tau_c}^{\tau_h} \tau d\tau (1 - f) e^{i\tau[\frac{K_T}{E_K} q_T \cos \alpha \cosh y + q_L (\frac{K_L}{E_K} \cosh y - \sinh y)]} e^{-\frac{1}{T_c} (E_K \cosh y - K_L \sinh y)} + \\
& \int_{\tau_h}^{\tau_f} \tau d\tau e^{i\tau[\frac{K_T}{E_K} q_T \cos \alpha \cosh y + q_L (\frac{K_L}{E_K} \cosh y - \sinh y)]} \\
& \exp \left[ -\frac{1}{T_c} (E_K \cosh y - K_L \sinh y) \left( \frac{\tau}{\tau_h} \right)^{1/3} e^{\kappa(\tau - \tau_h)/(2R_T)} \right] \} + \\
\mathcal{F} & \langle \rho(y) \rangle C_\tau \tau_f \int_0^{2\pi} d\phi \int_0^{R_T} r_T dr_T \int_{-\infty}^{+\infty} dy [E_K \cosh y - K_L \sinh y] \\
& e^{i\tau[\frac{K_T}{E_K} q_T \cos \alpha \cosh y + q_L (\frac{K_L}{E_K} \cosh y - \sinh y)] - iq_T R_T \cos(\alpha - \phi)} e^{-\frac{1}{T_f} (E_K \cosh y - K_L \sinh y)} . \quad (36)
\end{aligned}$$

The five terms composing the correlation function represent, respectively, the emission from the quark and gluon initial stage, their contribution during the mixed phase, the pion emission also from the surface in that phase, the emission during the pure pionic phase up to reaching the freeze-out temperature,  $T_f$ , and finally, the volumetric instantaneous decoupling once it was reached. Since the HBT correlation is among identical particles, we have considered also the fraction  $\left(\frac{g_{QGP}}{g_\pi}\right)$  of the QGP degrees of freedom converted into one species of pions only. We should also notice that the last term in Eq. (36) is weighted by the factor  $\mathcal{F}$ , given in Eq. (35) and in Table 2 (for  $\kappa = 1$ ), which takes into account the remnant part of the system at breakup.

Similarly, we can write the spectrum, as

$$\begin{aligned}
G(k_i, k_i) = & \langle \rho(y) \rangle C_\tau R_T \int_{-\frac{\pi}{2}}^{\frac{\pi}{2}} d\phi \cos \phi \int_{-\infty}^{+\infty} dy [E_i \cosh y - k_{iL} \sinh y] \\
& \left\{ \frac{g_{QGP}}{g_\pi} \int_{\tau_0}^{\tau_c} \tau d\tau \exp\left[-\frac{1}{T_0}(E_i \cosh y - k_{iL} \sinh y)\left(\frac{\tau}{\tau_0}\right)^{1/3} e^{\kappa(\tau-\tau_0)/(2R_T)}\right] + \right. \\
& \frac{g_{QGP}}{g_\pi} \int_{\tau_c}^{\tau_h} \tau d\tau (f) e^{-\frac{1}{T_c}(E_i \cosh y - k_{iL} \sinh y)} + \int_{\tau_c}^{\tau_h} \tau d\tau (1-f) e^{-\frac{1}{T_c}(E_i \cosh y - k_{iL} \sinh y)} + \\
& \left. \int_{\tau_h}^{\tau_f} \tau d\tau \exp\left[-\frac{1}{T_c}(E_i \cosh y - k_{iL} \sinh y)\left(\frac{\tau}{\tau_h}\right)^{1/3} e^{\kappa(\tau-\tau_h)/(2R_T)}\right] \right\} + \mathcal{F} \langle \rho(y) \rangle C_\tau \tau_f \\
& \times \int_0^{2\pi} d\phi \int_0^{R_T} r_T dr_T \int_{-\infty}^{+\infty} dy [E_i \cosh y - k_{iL} \sinh y] e^{-\frac{1}{T_f}(E_i \cosh y - k_{iL} \sinh y)}. \quad (37)
\end{aligned}$$

For estimating the (real) amplitudes  $G(k_i, k_i)$  in the denominator of Eq. (1), we wrote  $\mathbf{k}_1 = \mathbf{K} + \mathbf{q}/2$  and  $\mathbf{k}_2 = \mathbf{K} - \mathbf{q}/2$ , from the definition of the momenta  $\mathbf{K}$  and the relative momentum  $\mathbf{q}$ , since we are not generating the individual momenta and later averaging over all of them, as done in the experiment. In this first approach, that is the way we connected the momenta  $k_i$  in the spectra  $C(k_i, k_i)$  to the momenta appearing in the complex amplitude,  $C(k_1, k_2) = C(q, K)$ .

This means that we can write

$$|\mathbf{k}_{\mathbf{T}1,2}| = \sqrt{(\mathbf{K}_T \pm \mathbf{q}_T/2)^2} = \sqrt{\mathbf{K}_T^2 + \frac{\mathbf{q}_T^2}{4} \pm K_T q_T \cos \alpha}. \quad (38)$$

$$|\mathbf{k}_{\mathbf{L}1,2}| = \sqrt{K_L^2 + \frac{q_L^2}{4} \pm K_L q_L} ; E_{1,2} = \sqrt{m^2 + (\mathbf{K}_T \pm \mathbf{q}_T/2)^2 + (K_L \pm q_L/2)^2}. \quad (39)$$

In these equations,  $\alpha$  is the angle between  $\mathbf{K}_T$  and  $\mathbf{q}_T$ .

Due to the azimuthal symmetry of the problem, we can choose  $\mathbf{K}_T$  along the  $x$ -axis, without any loss of generality. In this way, we see that the so-called *outward* direction (defined by the component of  $\mathbf{q}_{T_o} \parallel \mathbf{K}_T$ ) will be along this direction and the *sideward* (defined by the component of  $\mathbf{q}_T \perp \mathbf{K}_T$ ), will be directed along the  $y$ -axis, i.e.,  $q_x = q_{T_o}$  and  $q_y = q_{T_s}$ . This implies that, in the first case, we chose  $\alpha = 0$  and, in the second,  $\alpha = \pi/2$ .

If we include the constant flow at the emission surface, the expressions for the complex amplitude,  $G(k_1, k_2)$  and the single-inclusive distributions,  $G(k_i, k_i)$  would be written as

$$\begin{aligned}
G(k_1, k_2) = & \frac{<\rho(y)> C_\tau R_T}{\sqrt{1-v_0^2}} \int_{-\frac{\pi}{2}}^{\frac{\pi}{2}} d\phi \cos \phi \int_{-\infty}^{+\infty} dy [E_K \cosh y - K_L \sinh y - v_0 K_T \cos \phi] \\
& \left\{ \frac{g_{QGP}}{g_\pi} \int_{\tau_0}^{\tau_c} \tau d\tau e^{i\tau[\frac{K_T}{E_K} q_T \cos \alpha \cosh y + q_L(\frac{K_L}{E_K} \cosh y - \sinh y)] - iq_T R_T \cos(\alpha - \phi)} \right. \\
& \exp \left[ -\frac{1}{T_0 \sqrt{1-v_0^2}} (E_K \cosh y - K_L \sinh y - v_0 K_T \cos \phi) \left( \frac{\tau}{\tau_0} \right)^{1/3} e^{\kappa(\tau-\tau_0)/(2R_T)} \right] + \\
& \frac{g_{QGP}}{g_\pi} \int_{\tau_c}^{\tau_h} \tau d\tau (f) e^{i\tau[\frac{K_T}{E_K} q_T \cos \alpha \cosh y + q_L(\frac{K_L}{E_K} \cosh y - \sinh y)] - iq_T R_T \cos(\alpha - \phi)} \\
& e^{-\frac{1}{T_c \sqrt{1-v_0^2}} (E_K \cosh y - K_L \sinh y - v_0 K_T \cos \phi)} + \int_{\tau_c}^{\tau_h} \tau d\tau (1-f) e^{-iq_T R_T \cos(\alpha - \phi)} \\
& e^{i\tau[\frac{K_T}{E_K} q_T \cos \alpha \cosh y + q_L(\frac{K_L}{E_K} \cosh y - \sinh y)]} e^{-\frac{1}{T_c \sqrt{1-v_0^2}} (E_K \cosh y - K_L \sinh y - v_0 K_T \cos \phi)} + \\
& \left. \exp \left[ -\frac{1}{T_c \sqrt{1-v_0^2}} (E_K \cosh y - K_L \sinh y - v_0 K_T \cos \phi) \left( \frac{\tau}{\tau_h} \right)^{1/3} e^{\kappa(\tau-\tau_h)/(2R_T)} \right] \right\} + \\
& \mathcal{F} <\rho(y)> C_\tau \tau_f \int_0^{2\pi} d\phi \int_0^{R_T} r_T dr_T \int_{-\infty}^{+\infty} dy [E_K \cosh y - K_L \sinh y] \\
& e^{i\tau[\frac{K_T}{E_K} q_T \cos \alpha \cosh y + q_L(\frac{K_L}{E_K} \cosh y - \sinh y)] - iq_T R_T \cos(\alpha - \phi)} e^{-\frac{1}{T_f} (E_K \cosh y - K_L \sinh y)}, \quad (40)
\end{aligned}$$

and the spectrum, as

$$\begin{aligned}
G(k_i, k_i) = & <\rho(y)> \frac{C_\tau R_T}{\sqrt{1-v_0^2}} \int_{-\frac{\pi}{2}}^{\frac{\pi}{2}} d\phi \cos \phi \int_{-\infty}^{+\infty} dy [E_i \cosh y - k_{iL} \sinh y - v_0 k_{iT} \cos \phi] \\
& \left\{ \frac{g_{QGP}}{g_\pi} \int_{\tau_0}^{\tau_c} \tau d\tau \exp \left[ -\frac{(E_i \cosh y - k_{iL} \sinh y - v_0 k_{iT} \cos \phi)}{T_0 \sqrt{1-v_0^2}} \left( \frac{\tau}{\tau_0} \right)^{1/3} e^{\kappa(\tau-\tau_0)/(2R_T)} \right] + \right. \\
& \frac{g_{QGP}}{g_\pi} \int_{\tau_c}^{\tau_h} \tau d\tau (f) e^{-\frac{1}{T_c \sqrt{1-v_0^2}} (E_i \cosh y - k_{iL} \sinh y - v_0 k_{iT} \cos \phi)} + \\
& \int_{\tau_c}^{\tau_h} \tau d\tau (1-f) e^{-\frac{1}{T_c \sqrt{1-v_0^2}} (E_i \cosh y - k_{iL} \sinh y - v_0 k_{iT} \cos \phi)} + \\
& \left. \int_{\tau_h}^{\tau_f} \tau d\tau \exp \left[ -\frac{(E_i \cosh y - k_{iL} \sinh y - v_0 k_{iT} \cos \phi)}{T_c \sqrt{1-v_0^2}} \left( \frac{\tau}{\tau_h} \right)^{1/3} e^{\kappa(\tau-\tau_h)/(2R_T)} \right] \right\} + \\
& \mathcal{F} <\rho(y)> C_\tau \tau_f \int_0^{2\pi} d\phi \int_0^{R_T} r_T dr_T \int_{-\infty}^{+\infty} dy [E_i \cosh y - k_{iL} \sinh y] e^{-\frac{1}{T_f} (E_i \cosh y - k_{iL} \sinh y)}. \quad (41)
\end{aligned}$$

We recall that, for estimating the (real) amplitudes  $G(k_i, k_i)$  in the denominator of Eq.(1), we used Eq. (38) and (39).

In order to check how the spectra estimated within our model and the above discussed relations behave compared to data, we plot the single-inclusive distribution in Fig. 3. From

here on we limit our estimates and discussions to the central rapidity region, i.e.,  $y_i = 0$  (which implies that  $k_{iL} = 0$ , and, consequently,  $K_L = 0$  and  $q_L = 0$ ). In Fig. 3, we show the spectra (in  $\text{GeV}^{-2}$ , within a constant arbitrary normalization) for the set of interrelated values shown in the first line of Table 2 and for two values of the flow velocity. The one that fits best the low transverse momentum region corresponds to no flow case,  $v_0 = 0$ . The other, to the flow velocity  $v_0 = 0.537$  [7], inspired by results at SPS. We see that the opposite happens in this case: the high transverse momentum region is better described by the case with flow than the low  $k_{iT} = 0$  region. We shall consider both these possibilities when studying the correlation function and fitted radii.

In Fig. 4 we show the correlation functions  $C(q_{To}) \propto q_{To}$  (solid curves), corresponding to  $\alpha = 0$ , and  $C(q_{Ts}) \propto q_{Ts}$  (dashed ones, very close to one another), for  $\alpha = \pi/2$ , in the same plot for better visualize the differences. The transverse flow was not introduced in those computations. When calculating the correlation function in terms of  $q_{To}$ , we fixed  $q_{Ts} = 0$  (remember that we had already fixed  $q_L = 0$ , as a simplifying assumption). They are displayed for three values of the average pair momentum,  $K_T = 0.17, 0.47$ , and  $0.80 \text{ GeV}/c$ . The oscillatory pattern seen for  $q_{To} \geq 0.05 \text{ GeV}/c$  is a result of the interference of the four first terms in Eq.(36) with the fifth term, which can be analytically integrated resulting in

$$\mathcal{F} 4\pi^2 \langle \rho(y) \rangle \propto C_\tau \tau_f R_T^2 M_T K_1 \left[ \frac{M_T}{T} - i\tau_f q_{To} \frac{K_T}{M_T} \right] \frac{J_1[q_{To} R_T]}{(q_{To} R_T)} , \quad (42)$$

in terms of the *outwards* component,  $q_{To}$ , with  $M_T = \sqrt{m^2 + \mathbf{K}_T^2}$ . The *sidewards* one,  $q_{Ts}$ , can be easily obtained from Eq. (42), by replacing  $q_{To} \rightarrow q_{Ts}$  and by replacing the argument of the first Bessel function by  $K_1\left(\frac{M_T}{T}\right)$ . Consequently, the behavior of the correlation functions, more evident in terms of  $q_{To}$ , represents an average over emission from the surface over the period  $\tau_0 \leq \tau \leq \tau_f$ , and the instantaneous volumetric emission at  $\tau = \tau_f$ . This “*averaging*” over different emission radii introduces a slight dependence of  $q_{Ts}$  in the average transverse momentum of the pair,  $K_T$ , more clearly visible in Fig. 5 that follows. In terms of the *outwards* component,  $q_{To}$ , we see that the correlation function depends more strongly on the transverse momentum, becoming broader (consequently, the width decreases) as  $K_T$  increases. This behavior is related to the restriction to forward emission from the opaque source considered in the first four terms of Eq. (36)-(37), and (40)-(41).

In Fig. 5, we illustrate the behavior of the correlation functions,  $C(q_{To}) \propto q_{To}$  (solid curves) and  $C(q_{Ts}) \propto q_{Ts}$  (dashed curves), when the flow ( $v_0 = 0.537$ ) is included, for the same values of  $K_T$ , as in Fig. 4. Similar behavior, but with more pronounced differences than in Fig. 4, is seen in Fig. 5.

Although not shown for sake of clarity in the plots, the correlation functions,  $C(q_{To}) \propto q_{To}$  and  $C(q_{Ts}) \propto q_{Ts}$ , were also computed for other three values of  $K_T$ , i.e., all together, for  $K_T = 0.17, 0.27, 0.38, 0.47, 0.63$ , and  $0.80 \text{ GeV}/c$ . Each of the curves, both for  $v_0 = 0$  and for  $v_0 = 0.537$ , were fitted by Gaussians, in the regions where their behavior could be reasonably well approximated to that shape. In this way, we obtained the corresponding average values of  $R_{out}$  and  $R_{sid}$ , as shown in Fig. 6 and 7, and from those, we estimated the ratio  $R_{out}/R_{sid}$ . We see that, for the no flow case,  $R_{sid}$  as a function of  $K_T$  is basically flat, but our  $R_{out}$  decreases with increasing  $K_T$ , although only slightly. The values obtained for the ratio are

plotted in Fig. 8 (for  $v_0 = 0$  and  $v_0 = 0.537$  cases), together with the preliminary STAR (filled triangles) and PHENIX (filled circles) data for both  $\pi^+$  and  $\pi^-$ . We can see that our results were extremely successful in describing both sets of data.

## VI. SUMMARY AND CONCLUSIONS

This simple model works well for the ratio of  $R_{out}/R_{sid}$  and suggests that the origin of the experimental value lies in the opacity of source emission. The model also describes the typical source radii reasonably well, but not the  $K_T$  dependence of these radii, as seen in Figs. 6 and 7. This suggests that time variation in either the magnitude of flow or the emitting radius may play a significant role, [12]- [14]. Also, a proper treatment of the the decoupling is not included in our computations and this certainly will affect the results, although it might also suggest modification in the treatment of decoupling, [14], [15].

At a minimum, these computations suggest that the problem in describing the various HBT ratios lies not so much in  $R_{out}/R_{sid}$  as it does in computing the full set of radii and obtaining a comprehensive and complete description of all of the above within one dynamical model. The ratio of  $R_{out}/R_{sid}$  may very well be independent of many of the variations within these models since it is dimensionless, where the dimensionful values of the various radii are sensitive to changes of time and size scales.

## ACKNOWLEDGMENTS

S.S.P. would like to express her gratitude to the Nuclear Theory Group at BNL for their kind hospitality and for the stimulating discussion atmosphere during the elaboration of this work. She would also like to thank R. Keith Ellis and the Theoretical Physics Dept. at Fermilab, for their kind hospitality. This research was partially supported by CNPq under Proc. N. 200410/82-2. This manuscript has been authored under Contracts No. DE-AC02-98CH10886 and No. DE-AC02-76CH0300 with the U.S. Department of Energy.

## REFERENCES

- [1] F. Laue, "HBT at RHIC", <http://www.rhic.bnl.gov/qm2001/program.html>, Proc. Quark Matter 2001; C. Alder et al., STAR Collab., Phys. Rev. Lett. 87 (2001) 082301.
- [2] Stephen Johnson: "RHIC, PHENIX, HBT and other acronyms", RHIC/INT Winter Workshop 2002 on "Correlations and Fluctuations in Heavy-Ion Collisions at RHIC", Seattle, Jan 4-6 2002; K. Adcox et al, nucl-exp/0201008.
- [3] H. Heiselberg and A. P. Vischer, Eur. Phys. J. C1 (1998) 593; H. Heiselberg, Phys. Lett. B421 (1998) 18.
- [4] For reviews on HBT, see Refs. [6] and [10] below, as well as: W.A. Zajc, Hadronic Multiparticle Production, World Scientific Press, P. Carruthers, ed. (1988); D.H. Boal, C.K. Gelbke and B.K. Jennings, Rev. Mod. Phys. 62 (1990) 553; C-Y. Wong, *Introduction to High-Energy Heavy-Ion Collisions*, World Scientific (1994); R.M. Weiner, *Bose-Einstein Correlations in Particle and Nuclear Physics*, J. Wiley & Sons (1997); U. Heinz and B. V. Jacak, Ann. Rev. Nucl. Part. Sci. 49 (1999) 529; T. Csörgő, Heavy Ion Phys. 15 (2002) 1-80.
- [5] S. Pratt, Phys. Rev. D33 (1986) 1314 ; Y. Hama and Sandra S. Padula, Phys. Rev. D37 (1988) 3237; G. F. Bertsch, Nucl. Phys. A498 (1989) 173c.
- [6] U. Heinz and B. Jacak, Ann. Rev. Nucl. Part. Sci. 49 (1999) 529.
- [7] B. Tomásik, U. A. Wiedermann, and U. Heinz, nucle-th/9907096.
- [8] R. A. Soltz, M. Baker, and J. H. Lee, Nucl. Phys. A661 (1999) 439c.
- [9] J. D. Bjorken, Phys. Rev. D27 (1983) 140.
- [10] M. Gyulassy, S.K. Kauffmann, and L.W. Wilson, Phys. Rev. C20 (1979) 2267; K. Kolehmainen and M. Gyulassy, Phys. Lett. B180 (1986) 203.
- [11] M. Gyulassy and Sandra S. Padula, Phys. Lett. B217 (1989) 181; Sandra S. Padula, M. Gyulassy and S. Gavin, Nucl. Phys. B329 (1990) 357 ; Sandra S. Padula and M. Gyulassy, Nucl. Phys. B339 (1990) 378.
- [12] U. Heinz and P. Kolb, hep-ph/0204061.
- [13] Tetsufumi Hirano, Keiichi Tsuda, Kohei Kajimoto, nucl-th/0011087.
- [14] D. Teaney, J. Lauret, Edward V. Shuryak Phys.Rev.Lett.86:4783-4786,2001.
- [15] S. A. Bass et al., Phys. Rev. C60 (1999) 21902.

## FIGURES

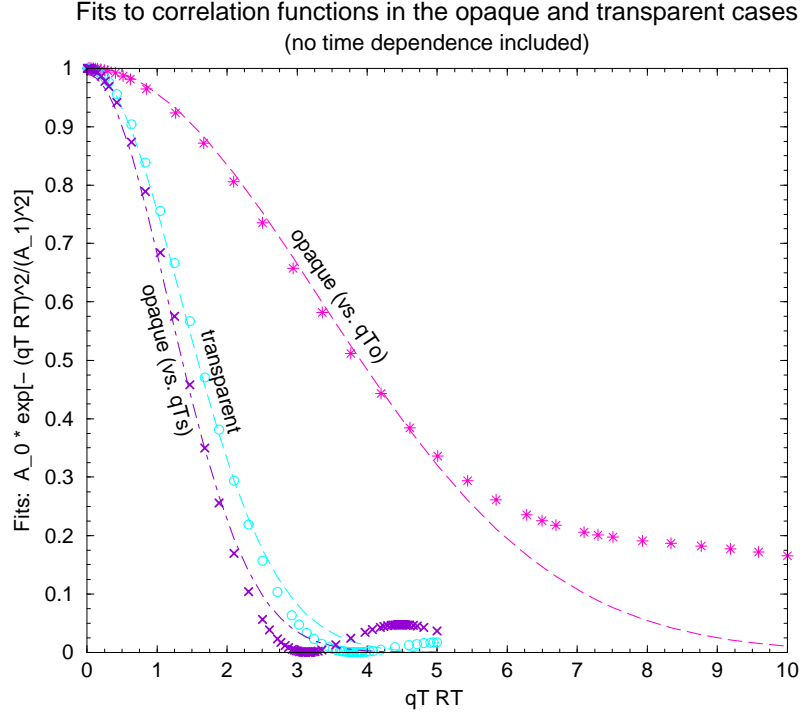


FIG. 1. Illustration of the correlation functions in the *very simple model* for  $R_{out}$  and  $R_{sid}$  as a function of the corresponding variable  $q_{T_o}$  and  $q_{T_s}$ . The set of points and curve in the middle correspond to both  $C(q_{T_o})$  vs.  $q_{T_o}$  and  $C(q_{T_s})$  vs.  $q_{T_s}$  in the transparent case, since **no** time dependence is included in the  $q_{T_o}$  variable in the above plot. On the other hand, the narrower and the wider sets correspond, respectively, to  $C(q_{T_s})$  vs.  $q_{T_s}$  and to  $C(q_{T_o})$  vs.  $q_{T_o}$  in the opaque case. We see that, as a result of the opacity of the source, this last set is much broader than the first one.

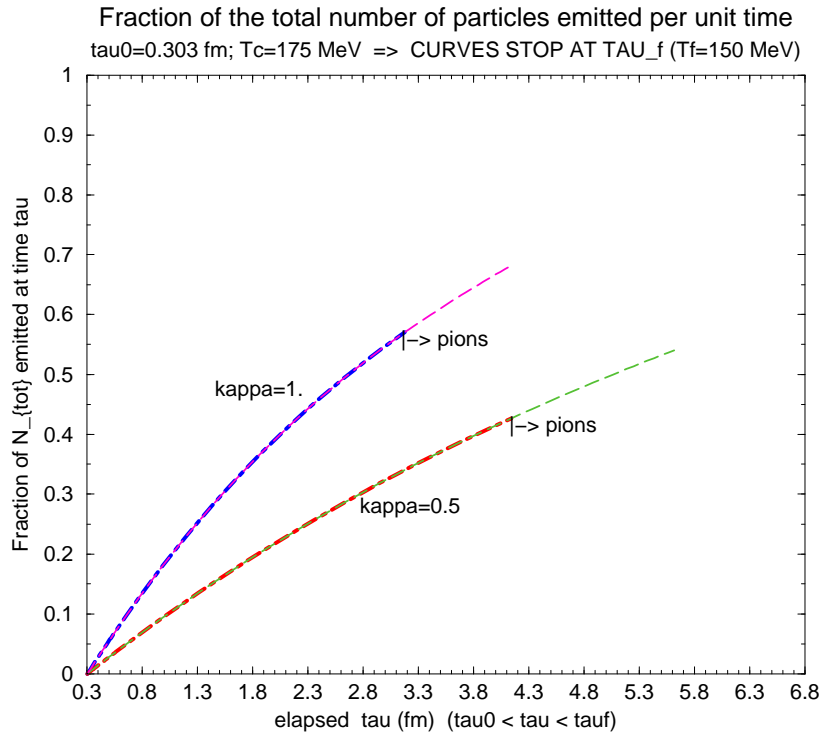


FIG. 2. The flux of emitted particles per unit time is shown, for two values of  $\kappa = 1$ , at each instant starting at  $\tau_0 = 0.303$  fm/c, passing by the beginning of the phase transition, at  $\tau = \tau_c$ , then through its end at  $\tau_h$ , and finally, stopping at the instant when the pionic system reaches  $\tau_f$ . We clearly see the fraction of the pions still in the system at that instant, which is then immediately emitted from the entire volume. In this example, we fixed  $T_0 = 217$  MeV,  $R_T \approx 7$  fm/c, and the number of quark flavors in the QGP phase to be 2.

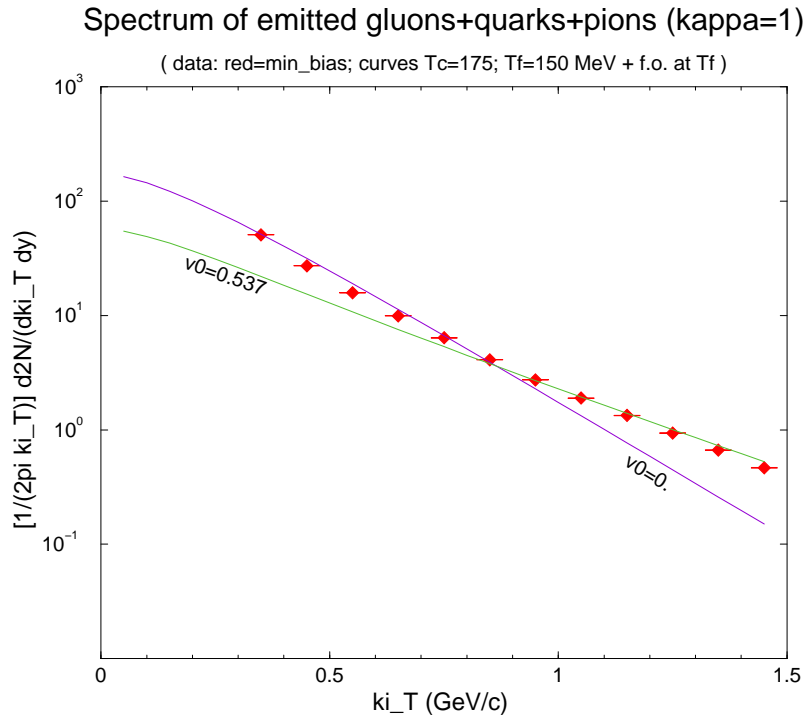


FIG. 3. The prediction based on our model for the transverse momentum distribution of emitted pions is shown. The points are from the minimum-bias data from PHENIX Collaboration. The two curves correspond to no flow ( $v_0 = 0$ ) and flow ( $v_0 = 0.537$ ) cases. The first describes data well in the low momentum region of the pions,  $k_{iT}$ , whereas the case including flow describes better the spectrum at large transverse momentum of the individual particles. The parameters used are explained in the text, corresponding to  $T_0 = 217$  MeV,  $T_c = 175$  MeV,  $T_f = 150$  MeV,  $\kappa = 1$ , and the transverse radius,  $R_T \approx 7$  fm/c.

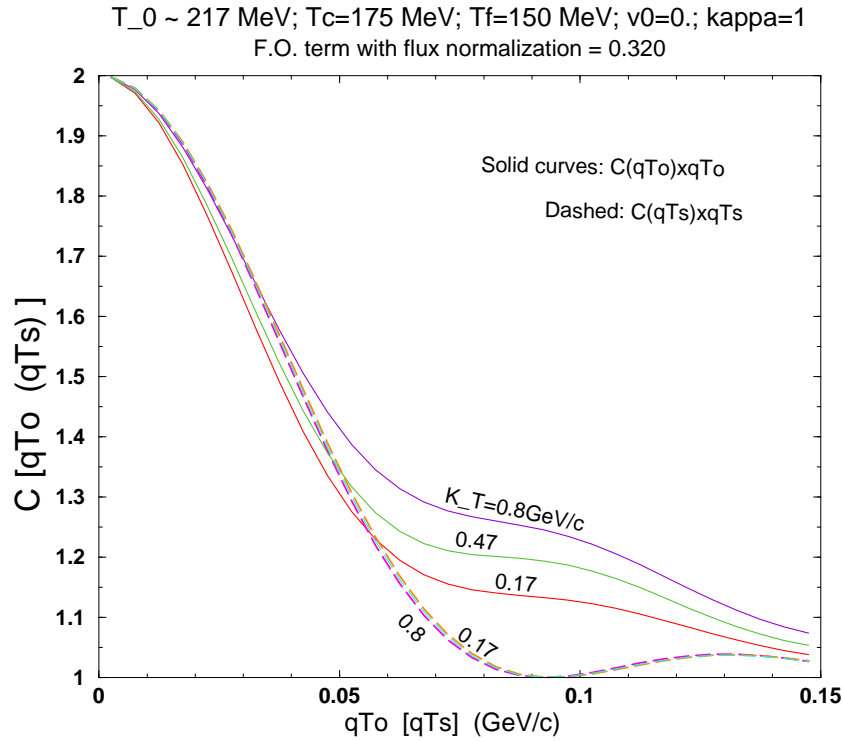


FIG. 4. The correlation functions,  $C(q_{To}, K_T)$  vs.  $q_{To}$  (solid), and  $C(q_{Ts}, K_T)$  vs.  $q_{Ts}$  (dashed), are shown for three distinct values of the average pair momentum,  $K_T$ , corresponding to the phase transition temperature  $T_c = 175 \text{ MeV}$ ,  $T_c = 150 \text{ MeV}$  including a volumetric emission when the hadronic (pions) system reaches  $\tau = \tau_f$ . We see that the width of the curves as function of  $q_{To}$  increase (or conversely, the radii decrease) with increasing  $K_T$ , whereas the curves for different  $q_{Ts}$  show very small variation, as would be expected since no flow is considered in this case. The same input parameters were adopted here:  $T_0 = 217 \text{ MeV}$ ,  $T_c = 175 \text{ MeV}$ ,  $T_f = 150 \text{ MeV}$ ,  $\kappa = 1$ , and the transverse radius,  $R_T \approx 7 \text{ fm/c}$ .

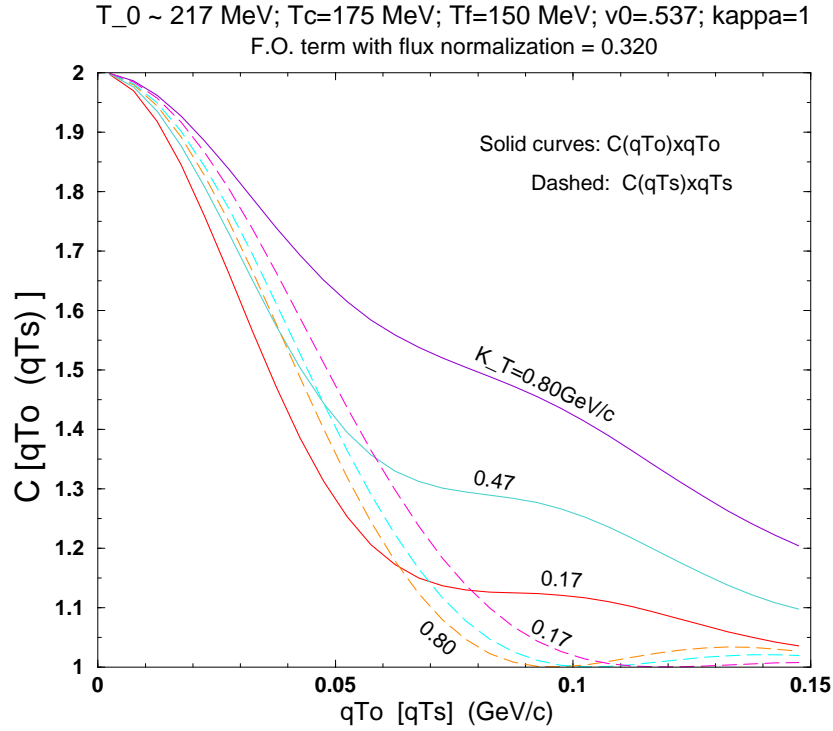


FIG. 5. The correlation functions,  $C(q_{T_o}, K_T)$  vs.  $q_{T_o}$  (solid), and  $C(q_{T_s}, K_T)$  vs.  $q_{T_s}$  (dashed), are shown for three distinct values of the average pair momentum,  $K_T$ , as Fig. 4. We see that the width of the solid curves, increase (or conversely, the radii decrease) with increasing  $K_T$ , since now a constant flow is considered. However, the opposite behavior is seen as a function of  $q_{T_s}$ . The same input parameters were adopted here:  $T_0 = 217 \text{ MeV}$ ,  $T_c = 175 \text{ MeV}$ ,  $T_f = 150 \text{ MeV}$ ,  $\kappa = 1$ , and the transverse radius,  $R_T \approx 7 \text{ fm}/c$ .

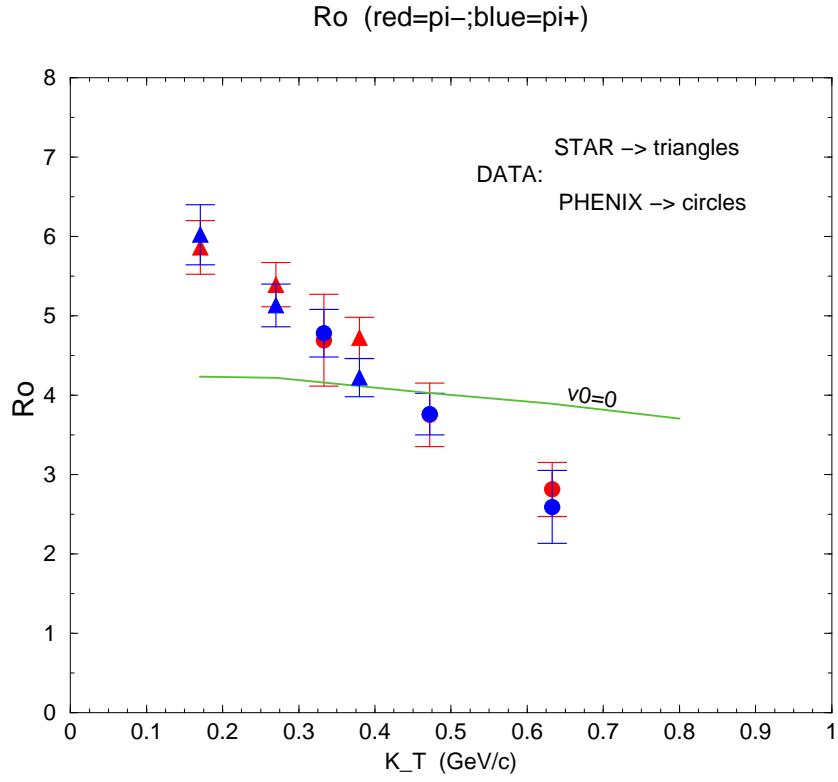


FIG. 6. Our results for  $R_{out}$  (outwards) radius are shown as a function of the average pair momentum,  $K_T$ , when no flow ( $v_0 = 0$ ) is considered. The experimental data points from STAR (triangles) and PHENIX (circles) are also included in the plot. The values of the parameters are the same as in the previous plots, i.e.,  $T_0 = 217$  MeV,  $T_c = 175$  MeV,  $T_f = 150$  MeV,  $\kappa = 1$ , and the transverse radius,  $R_T \approx 7$  fm/c.

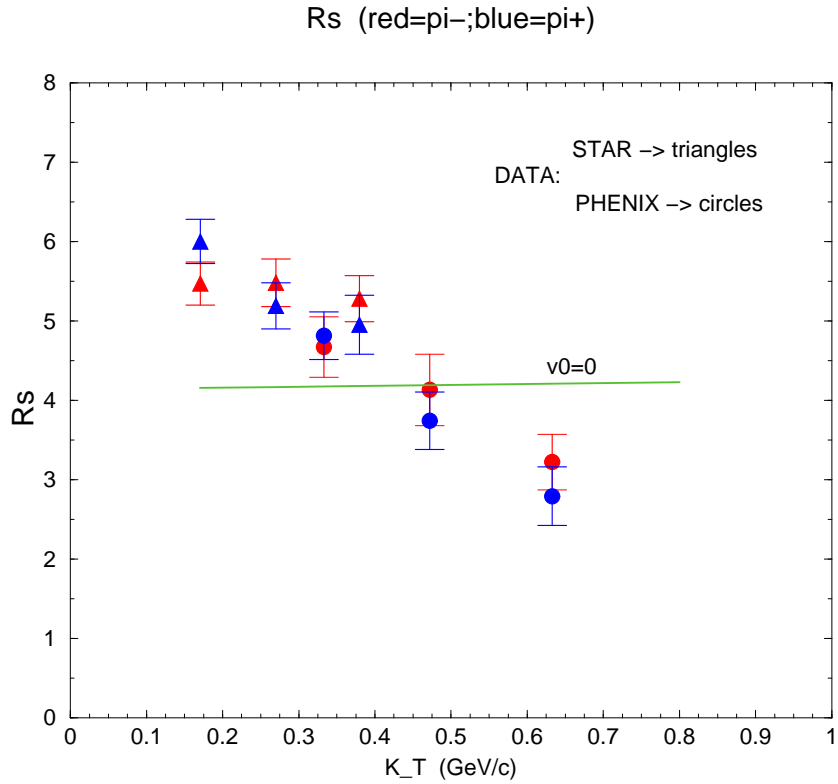


FIG. 7. The results for  $R_{sid}$  (sideways) radius vs.  $K_T$  are shown for the no flow ( $v_0 = 0$ ) case. The experimental data points with error bars are from STAR (triangles) and PHENIX (circles). The values of the parameters are the same as in the previous plots, i.e.,  $T_0 = 217$  MeV,  $T_c = 175$  MeV,  $T_f = 150$  MeV,  $\kappa = 1$ , and the transverse radius,  $R_T \approx 7$  fm/c.

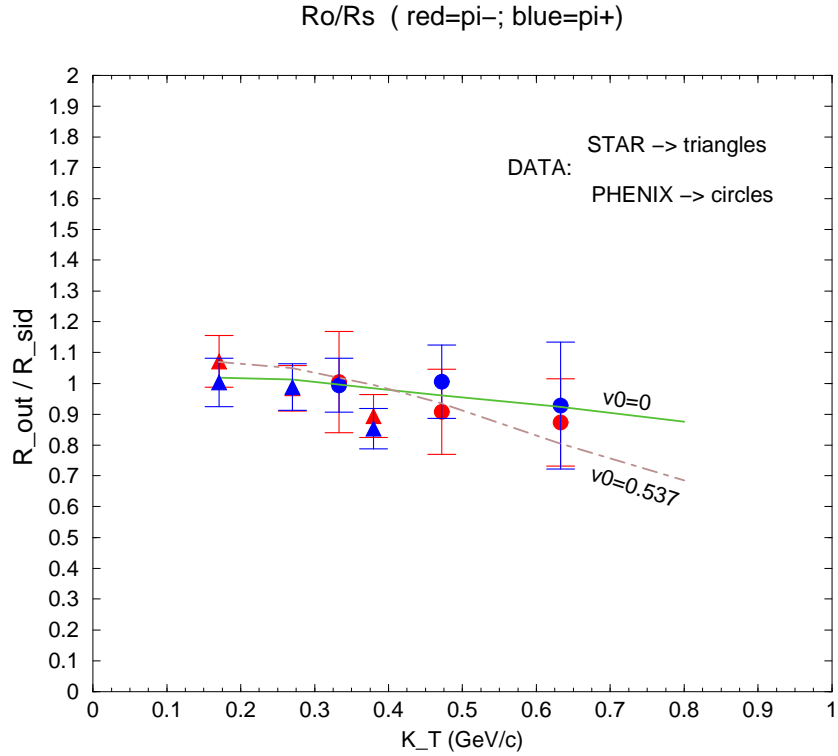


FIG. 8. The result corresponding to the ratio  $R_{out}/R_{sid}$  of the *outwards* radius by the *side-wards* one is shown within the Tamale Model. We see that **both** values of the flow velocity considered, i.e.,  $v_0 = 0$ . and  $v_0 = 0.537$  result into values of the ratio that agree very well with data within the experimental error bars (shown in the plot). The values of the parameters are the same as in the previous plots, i.e.,  $T_0 = 217$  MeV,  $T_c = 175$  MeV,  $T_f = 150$  MeV,  $\kappa = 1$ , and the transverse radius,  $R_T \approx 7$  fm/c.